

## A NOVEL INDEX OF ABUNDANCE OF JUVENILE YELLOWFIN TUNA IN THE INDIAN OCEAN DERIVED FROM ECHOSOUNDER BUOYS

Josu Santiago<sup>1</sup>, Jon Uranga<sup>2</sup>, Iñaki Quincoces<sup>1</sup>, Blanca Orue<sup>2</sup>, Maitane Grande<sup>2</sup>, Hilario Murua<sup>2,3</sup>, Gorka Merino<sup>2</sup>, Agurtzane Urtizbered<sup>2</sup>, Pedro Pascual<sup>4</sup>, Guillermo Boyra<sup>2</sup>

### SUMMARY

*The collaboration with the Spanish vessel-owners associations and the buoy-providers companies, has made it possible the recovery of the information recorded by the satellite linked GPS tracking echosounder buoys used by the Spanish tropical tuna purse seiners and associated fleet in the Indian Ocean since 2010. These instrumental buoys inform fishers remotely in real-time about the accurate geolocation of the FAD and the presence and abundance of fish aggregations underneath them. Apart from its unquestionable impact in the conception of a reliable CPUE index from the tropical purse seine tuna fisheries fishing on FADs, echosounder buoys have also the potential of being a privileged observation platform to evaluate abundances of tunas and accompanying species using catch-independent data. Current echosounder buoys provide a single acoustic value without discriminating species or size composition of the fish underneath the FAD. Therefore, it has been necessary to combine the echosounder buoys data with fishery data, species composition and average size, to obtain a specific indicator. This paper presents a novel index of abundance of juvenile yellowfin tuna in the Indian Ocean derived from echosounder buoys for the period 2010-2018, with the aim of contributing to the 2019 assessment of this stock..*

### 1. Introduction

Fishery stock assessment models are demographic analyses designed to determine the effects of fishing on fish populations and to evaluate the potential consequences of alternative harvest policies (Methot & Wetzel, 2012). Quantification of fish populations is the central part of any fish stock assessment and it is commonly the most difficult task. This is even more complicated in the case of highly migratory fish stocks, such as tuna, where conventional fishery-independent surveys are in general not practicable. And, in the absence of fishery-independent information, most of the abundance indices used in fish stock assessments are derived from estimates of Catch per Unit Effort (CPUE), the number or biomass of fish caught as a function of effort (Quinn & Deriso, 1999).

Relative abundance indices based on CPUE data are notoriously problematic (Maunder et al., 2006), as catch data is usually biased by fishing effort, coverage, and other limiting factors of fishery data. The primary assumption behind a CPUE-based abundance index is that changes in the index are assumed to be proportional to changes in the actual stock abundance (Maunder & Punt, 2004), being catchability ( $q$ ) -the portion of the stock captured by one unit of effort - the coefficient of proportionality. One of the associated difficulties is that  $q$  is rarely constant and depends on several different components, such as those related to changes in the fishing efficiency and dynamics of the fleet.

Tropical tuna purse seining is one of such fisheries where both factors, fishing efficiency and dynamics of the

---

<sup>1</sup> AZTI, Marine Research Division, Txatxarramendi ugarte a z/g, 48395 Sukarrieta, Basque Country (Spain)

<sup>2</sup> AZTI, Marine Research Division, Herrera Kaia-Portu aldea z/g, 20110 Pasaia, Basque Country (Spain)

<sup>3</sup> ISSF, International Seafood Sustainability Foundation, Washington DC (USA), (current affiliation)

<sup>4</sup> IEO, C.O. de Canarias, Vía Espaldón, Dársena Pesquera, Parcela 8, 38180 Santa Cruz de Tenerife, Canary Islands (Spain)

fleet, are evolving very rapidly due to the fast technological development (Torres-Irineo et al, 2014) and the sharp increase of the use of Fish Aggregating Devices (FADs) (Scott & Lopez, 2014). This fact makes it difficult to obtain reliable CPUE indices for tropical tunas from purse fisheries fishing under drifting FADs. Recent initiatives such as the EU funded projects RECOLAPE, CECOFAD-1 and CECOFAD-2 are focusing on the understanding of the use of FADs in tropical purse seine tuna fisheries and to try to provide reliable estimates of abundance indices (Gaertner et al., 2016). And science-industry collaboration in the context of these and other projects is clearly improving the understanding of the FAD use but also the availability of data with great potential for improving CPUE indices and for developing novel abundance indicators.

The collaboration with the Spanish vessel-owners associations (ANABAC and OPAGAC) and the buoy-providers companies (Marine Instruments, Satlink and Zunibal), has made it possible the recovery of the information recorded by the satellite tracking echosounder buoys used by the Spanish tropical tuna purse seiners and associated fleet in the Indian Ocean for the period 2010-2018. These instrumental buoys inform fishers remotely in near real-time about the accurate geolocation of the FAD and the presence and abundance of tuna aggregations underneath them.

Apart from its unquestionable impact in the conception of a reliable CPUE index from the purse seine tropical tuna fisheries fishing on FADs, echosounder buoys have also the potential of being a privileged observation platform to evaluate abundances of tunas and accompanying species using catch-independent data (Dagorn et al., 2006; Lopez et al., 2014; Santiago et al., 2016).

Current echosounder buoys provide a single acoustic value without discriminating species or size composition of the fish underneath the FAD. Therefore, it has been necessary to combine the echosounder buoys data with fishery data, species composition and average size, to obtain species specific acoustic biomass indicators. This paper presents a novel index of abundance of juvenile yellowfin tuna in the Indian Ocean derived from echosounder buoys for the period 2010-2018.

An equivalent index, developed using the methodology described here, was presented for the 2019 stock assessment of Atlantic yellowfin (ICCAT, 2019a). In this assessment, the final uncertainty grid (with 4 different stock assessment scenarios) used to provide historical trends, current stock status and reference points using Stock Synthesis (Methot and Wetzel, 2012; ICCAT, 2019b) includes the BAI index. Depending on the scenario of the uncertainty grid of the ICCAT YFT assessment, the BAI index was used in conjunction with a joint longline index (Hoyle et al, 2019) and a free school purse seine index (Guéry et al. 2019). The longline and free school indices reflect the abundance of adult fish while the index proposed here is a recruitment-juvenile index. Therefore, we present BAI as a contribution to improve the Indian Ocean yellowfin stock assessment.

## **2. Material and methods**

### ***2.1 The acoustic data***

Acoustic data from echosounder buoys used in this analysis have been provided by the company Satlink. This type of buoy is equipped with a sounder, which operates at a frequency of 190.5 kHz with a power of 100 W. The range extends from 3 to 115 m, with a transducer blanking zone running from 0 to 3 m. At an angle of 32°, the cone of observation under the buoy has a diameter of 78.6 m at a depth of 115 m. The echosounder provides acoustic information in 10 different vertical layers, each with a resolution of 11.2 m. During the period analysed three different buoy models have been used by the fleet: DS+, DSL+ and ISL+. These three buoy models work with similar beam angle, frequency and power, and with the above mention vertical stratification. DSL+ and DS+ obtain three acoustic records per day, i.e. before dawn, at dawn and after dawn in the default mode. ISL+ has the capacity to sample along the day each 15 minutes, transmitting the signal if the value recorded for a 24 hours period is larger than the previous record.

The fishing companies belonging to ANABAC and OPAGAC that have provided acoustic information from their echosounder buoys were: Albacora, Atunsa, Atunsa INC, Comp Europea de Tunidos, Echebatar fleet, Hartswater, Inpesca, Inpesca Fishing, Interatun and Isabella Fishing. This adds up to a total of 25 purse seine vessels from 2 different flags (Spain and Seychelles) operating in the IOTC convention area.

The database of acoustic information of the Indian Ocean from Satlink buoys comprises around 10.9 million of records from over 64,741 buoys for the period from January 2010 to December 2018. The information on buoy positions and acoustic information is received in two different data-sets with the following fields:

- Data-set on buoy positions
  - o *Date*: Date of the last position of the day
  - o *Time*: Hour (GMT)

- *Buoy code*: Unique identification number of the buoy, given by the model code (D+, DS+, DL+, DSL+, ISL+, ISD+ followed by 5-6 digits).
  - *Latitude*: Latitude of the last position of the day (in decimals)
  - *Longitude*: Longitude of the last position of the day (in decimals)
  - *Velocity*:  $v$  calculated from the distance/time between the last position of the day and the last position of the previous day.
  - *Notes*: Empty column
- Data-set on acoustic records
- *Name*: Unique identification number of the buoy, given by the model code (D+, DS+, DL+, DSL+, ISL+, ISD+ followed by 5-6 digits).
  - *OwnerName*: Name of the buoy owner assigned to a unique purse seine vessel
  - *MD*: Message descriptor (160, 161 and 162 for position data, without sounder data, and 163, 168, 169 and 174 for sounder data)
  - *StoredTime*: Date (dd/mm/yyyy) and hour (H:MM) of the echosounder record
  - *Latitude, Longitude*: Not provided (this information is provided in the position data-set)
  - *Bat*: Not provided. (Charge level (in percentage). Except for the D+ and DS+ in voltage)
  - *Temp*: Temperature (Not provided)
  - *Speed*: Speed in knots (Not provided)
  - *Drift*: bearing in degrees (Not provided)
  - *Layer1-Layer10*: Depth observation range extends from 3 to 115 m, which is split in ten homogeneous layers, each with a resolution of 11.2 m. The buoy has also a blanking zone (a data exclusion zone to eliminate the near-field effect of the transducer between 0 and 3 m. 32 pings are sent from the transducer and an average of the backscattered acoustic response is computed and stored in the memory of the buoy. Manufacturer's method converts raw acoustic backscatter into biomass in tons, using a depth layer echo-integration procedure based exclusively on an algorithm based on the TS and weight of skipjack tuna.
  - *Sum*: Sum of the biomass estimated at each layer
  - *Max*: Maximum biomass estimated at any layer
  - *Mag1, Mag3, Mag5 and Mag7*: Magnitudes corresponding to the counts of detected targets according to the TS of the detection peak.

## 2.2 From acoustic data to a species-specific abundance indicator

To calculate the biomass aggregated under a FAD from the acoustic signal, Satlink uses the density of one species, skipjack, to provide the biomass in tons, biomass data from Satlink was converted to decibels reversing their formula for the biomass computation. Then we recomputed biomass using standard abundance estimations equations (Simmonds & MacLennan, 2005):

$$Biomass_i = \frac{s_V \cdot Vol \cdot p_i}{\sum_i \sigma_i \cdot p_i}$$

where  $Vol$  is the sampled volume and  $p_i$  and  $\sigma_i$  are the proportion and linearized target strength of each species  $i$  respectively. Species proportions in weight were extracted from IOTC nominal catch reported by the EU fleet for each  $1^\circ \times 1^\circ$  and month stratum, as explained below. Mean fish lengths ( $L_i$ ) used for skipjack (SKJ), bigeye (BET) and yellowfin (YFT) were 48, 47 and 46 cm respectively<sup>5</sup>, and weights were obtained using weight-length relationships (IOTC conversion factors). Then, the following TS-length relationships were used to obtain linearized target strength per kilogram:

$$\sigma_i = \frac{10^{(20 \log(L_i) + b_{20,i})/10}}{w_i}$$

---

<sup>5</sup> Mean length values used at this stage are preliminary. In further revisions of the document the idea is to work with mean lengths of the PS FAD fishery catches by finer spatial-temporal strata.

Where  $w_i$  is the mean weight of each species. Given that each brand uses different operating frequencies, we used different b20 values for each. For Satlink, the b20 values were obtained from (Boyra et al., 2018) for SKJ and (Oshima, 2008) for YFT and BET.

Since all acoustic data is not covered with a corresponding species distribution data from EU PS nominal catch for each 1°x1° and month stratum, buoy distributions and species composition at the same 1°x1° grid, year and month were filtered and used in the analysis. The rest of the acoustic observations were not considered.

### 2.3 Acoustic data cleaning and filtering

Data cleaning included the removal of records without acoustic information (records with only position, speed and velocity), outliers (invalid, impossible or extreme values) related to bad geolocation, time, or other general variables. And aside of the regular exclusions due to this type of inconsistencies, the following considerations were also taken into account for accepting the data for the standardization analysis:

- Vertical boundary between tuna and non-tuna species: acoustic information from the shallower layers, <25m, was not considered for the analysis. According to (Lopez et al., 2017; Robert et al., 2013), the vertical boundary between non-tuna species and tunas can be considered at about 25 m. Excluding the first layers, we try to eliminate noise from the non-tuna species associated to the FAD.
- Bottom depth: Using high resolution bathymetry data (British Oceanographic Data Centre, UK, www.gebco.net), acoustic records from buoys located in areas with a bottom depth shallower than 200 m were excluded. The rationale of this exclusion is not to incorporate acoustic records of FADs that have drifted to coastal areas where tunas are less likely to be present.
- Acoustic measurements at sea: Buoys are normally turned on before deployment, so some records may correspond to onboard buoys. To deal with this issue we developed a Random Forest (RF) model (Orue et al., 2019) to classify the buoys at sea and onboard using information from Zunibal buoys. These buoys have the capability to identify between positions at sea or onboard, using a conductivity sensor. The sensor measures the current between two electrodes and through a simple algorithm it determines whether the Zunibal buoy is inside or outside the water. Those records classified as onboard were excluded.
- Time of the day: Only those samples obtained around sunrise, between 4 a.m. and 8 a.m., were considered for the analysis. These samples are supposed to capture the echosounder biomass signals that better represent the abundance of fish under the FADs, as this is the time when tuna is observed to be more closely aggregated around the FADs (Brill et al., 1999; Josse et al., 1998; Moreno et al., 2007). For the specific case of comparing the acoustic data with abundance it is important that the echosounder measurements are received when the signal is more representative of the biomass around the FAD model (Orue et al., 2019).
- Days since deployment: The objective of this selection criterion was to consider those acoustic records that were more likely associated to FAD trajectory, termed “virgin segments”.

A virgin segment is defined as the segment of a buoy trajectory whose associated FAD likely represents a new deployment which has been potentially colonized by tuna and not already fished. Orue et al. (2019) concluded that tuna seemed to arrive at FADs in  $13.5 \pm 8.4$  days and, thus, we consider as virgin segments (i.e. when tuna has aggregated to FAD) those segments of trajectories from 20-35 days at sea.

In order to identify and separate those segments and their acoustic samples, the overall trajectories of the entire life-time of each buoy were fractioned in smaller sequences corresponding to periods where they could have been attached to different FADs. A new sequence of a buoy was considered to occur, and hence an attachment to a new FAD, when the difference between two consecutive observations of the same buoy was larger than 30 days. Each sequence was assigned with a “new trajectory code” that included the code of the buoy plus the consecutive number of the sequence of each buoy. A deployment/redeployment of a buoy was considered to occur when the “new trajectory code” appears for the first time in the database.

Sequences with less than 30 observations were excluded from the analysis. Sequences having a time difference between any of the consecutive observations longer than 4 days during the first 35 days were also excluded.

Figure 1 shows a diagram with an example of “virgin” segments used for the calculation of the BAI index.

- Detection threshold: Acoustic records equal or less than 0,1 tonnes were considered zeros. This is a conservative preliminary value since further validation is needed.

## 2.4 The BAI index: Buoy-derived Abundance Index

The estimator of abundance BAI was defined as the 0.9 quantile of the integrated acoustic energy observations in each of the "virgin" sequences. A high quantile was chosen because the large values are considered to be likely produced by tuna (in opposition to plankton or bycatch species). This assumption is followed by all the buoy brands in the market, which use the maximum value as the summary of each time interval. In our case we selected a high quantile instead of the maximum to try to provide a more robust estimator by avoiding eventual outlier values. We did this to avoid taking into account the expected lowest values that might appear after eventual hauls occurring along the sequence. The total number of "virgin" sequences analysed, and hence the number of observations in the model, rose to 29,855, of which 28,300 (94.79%) were positives.

## 2.5 Covariates

Covariates included year-quarter (yyqq), and 5°x5° IOTC areas fitted as categorical variables. Other variables used in the standardization process included velocity of the buoy, FAD densities and a set of environmental variables. They were chosen for potential effects on the horizontal-vertical distribution of tunas and their association to FADs (FAD density, mixed layer height, sea surface temperature, chlorophyll concentration and detected fronts in sea surface temperature and chlorophyll daily datasets computed with Belkin and O'Reilly method) or on the quality of the echosounder measurements (buoy velocity). These variables were incorporated in the model as continuous variables.

A proxy of 1°x1° and monthly FAD densities were calculated as the average number of buoys over each month by summing up the total number of active buoys recorded per day over the entire month and dividing by the total number of days.

The environmental variables evaluated in the model were:

- Ocean mixed layer thickness: defined as the depth where the density increase compared to density at 10 m depth corresponds to a temperature decrease of 0.2°C in local surface conditions (θ10m, S10m, P0= 0 db, surface pressure).
  - o Source: Copernicus Marine Environment Monitoring Service (<http://marine.copernicus.eu>)
  - o Product: GLOBAL\_REANALYSIS\_PHY\_001\_030
  - o Update frequency: Yearly
  - o Available time series: 04/12/1992 to 27/12/2018
  - o Temporal resolution: daily mean
  - o Horizontal resolution: 1/12 ° (equirectangular grid)
  - o Units: [m]
- Chlorophyll: Mass concentration of chlorophyll a in sea water (depth = 0).
  - o Source: Copernicus Marine Environment Monitoring Service (<http://marine.copernicus.eu>)
  - o Product: GLOBAL\_REANALYSIS\_BIO\_001\_029
  - o Available time series: 1993/01/01 up to 2018/12/31
  - o Temporal resolution: daily mean
  - o Horizontal resolution: 1/4 ° (equirectangular grid)
  - o Units: [mg.m-3]
- Sea Surface Temperature (SST):
  - o Source: Multi-scale Ultra-High-Resolution Sea Surface Temperature (<https://mur.jpl.nasa.gov>)
  - o Product: JPL\_OUROCEAN-L4UHfnd-GLOB-G1SST
  - o Available time series: 2010/01/01 up to present
  - o Target delivery time: daily
  - o Temporal resolution: daily mean
  - o Horizontal resolution: Regular 0.01-degree grid
  - o Units: Kelvin degrees

SST and Chlorophyll fronts: Oceanographic front detection was performed using the "grec" package for R for each daily dataset, that provides algorithms for detection of spatial patterns from oceanographic data using image processing methods based on Gradient Recognition (Belkin & O'Reilly, 2009).

Figure 2 shows an example of one month of data, January 2017, of buoy trajectories, density of buoys by 1°x1° rectangles and environmental variables incorporated in the GLM analysis.

## 2.6 The model

The model we propose is based in an assumption very similar to the fundamental relationship among CPUE and abundance widely used in quantitative fisheries analysis. In our case we built the index based on the assumption that the signal from the echosounder is proportional to the abundance of fish.

$$BAI_t = \varphi \cdot B_t$$

where  $BAI_t$  is the Buoy-derived Abundance Index and  $B_t$  is the abundance in time  $t$  (Santiago et al., 2016).

Although it would appear to be obvious, there is not plenty of literature on the relationship between acoustic indicators and fishing performance. It is assumed that acoustic echo integration is a linear process, i.e., proportional to the number of targets (Simmonds & MacLennan, 2005) and has been experimentally proven to be correct with some limitations (Foote, 1983; Røttingen, 1976). Therefore, acoustic data (echo integration) is commonly taken as an estimator of abundance and is thoroughly applied to provide acoustic estimation of abundance of many pelagic species (e.g., Hampton, 1996; ICES, 2015; Massé, Uriarte, Angélico, & Carrera, 2018). So, does large biomass indicated by acoustic data consistently result in large catches when sets follow soon after? A recent study has found a positive significant correlation between echosounder acoustic energy and catches of tropical tuna around FADs (Moreno, et al., 2019). The study was based on data collected in two surveys conducted onboard commercial purse seiners during regular fishing activity in the Atlantic and Pacific Oceans in years 2014 and 2016. Simrad EK60 echosounders with split beam transducers at 38, 120 and 200 kHz were used to collect acoustic data. Generalized linear models were run between acoustic backscattering energy (NASC, MacLennan et al., 2002) and catches of the three main tuna species found at FADs (skipjack, bigeye and yellowfin) providing positive significant relationships with total catches (in weight) as well as catches for each tuna species.

As with the catchability, the coefficient of proportionality  $\varphi$  is not constant for many reasons. In order to ensure that  $\varphi$  can be assumed to be constant (i.e. to control the effects other than those caused by changes in the abundance of the population) a standardization analysis should be performed aiming to remove factors other than changes in abundance of the population. This can be performed standardizing nominal measurements of the echosounders using a Generalized Linear Mixed Modelling approach.

Considering the low proportion of zero values (5.21%) the delta lognormal approach (Lo et al., 1992) was not considered. GLMM (log-normal error structured model) was applied to standardize the acoustic observations. A stepwise regression was applied to the model with all the explanatory variables and interactions in order to determine those that significantly contributed to explain the deviance of the model. For this, deviance analysis tables were created for the positive acoustic records. Final selection of explanatory factors was conditional to: a) the relative percentage of deviance explained by adding the factor in evaluation (normally factors that explained more than 5% were selected), and b) The Chi-square ( $\chi^2$ ) significance test. Those factors that explained less than 5% of the variability of the model were not considered.

Interactions of the temporal component (year-quarter) with the rest of the variables were also evaluated. If an interaction was statically significant, it was then considered as a random interaction(s) within the final model (Maunder & Punt, 2004).

Lastly, the selection of the final mixed model was based on the Akaike's Information Criterion (AIC), the Bayesian Information Criterion (BIC), and a Chi-square ( $\chi^2$ ) test of the difference between the log-likelihood statistic of different model formulations. The year-quarter effect least square means (LSmeans) use a weighted factor of the proportional observed margins in the input data to account for the non-balance characteristics of the data. The LSMeans were bias corrected for the logarithm transformation algorithms using Lo et al (1992). All analyses were done using the lme4 package for R (Bates et al., 2015).

## 3. Results

A total of 10.9 million of records from over 64,741 buoys for the period from January 2010 to December 2018 were integrated into 29,855 observations for the GLM analysis. Each observation was calculated as the 90% percentile of a "virgin" segment of buoy trajectories. A virgin segment was defined as the segment of a buoy trajectory from 20-35 days at sea, so that the associated FAD likely represents a new deployment which has been potentially colonized by tuna and not already fished.

In this analysis we have obtained from the acoustic signal of the echosounder buoys associated to FADs the biomass of yellowfin tuna aggregated under a FAD. The aggregations of yellowfin tuna associated with floating objects are mostly composed of small individuals (FL around 46cm). Therefore, the Buoy-derived Abundance Index (BAI) would represent an indicator of YFT juvenile; a modal size of 46cm would correspond to around 1 year of life (Murua et al., 2017).

Figure 3 shows the histograms of the BAI and log transformed BAI nominal values. Log transformation makes the data to follow a normal distribution, as shown in the left panel of Figure 3. Figure 4 shows the spatial distribution [5°x5°] of the number of “virgin” sequences of buoy trajectories that have been used in the GLM analysis. The quarterly evolution of the number of observations on a 5°x5° grid is shown in Figure 5. The number of observations available has grown considerably over the years, especially since 2013.

Figure 6 shows a tableplot of the variables used in the GLM analysis. Independent variables tested in the GLM were year-quarter (yyqq), 5°x5° area (area), buoy model (model), buoy velocity (vel), FAD density (den), chlorophyll concentration (chl), detected fronts in chlorophyll (chlfront), sea surface temperature (sst), detected fronts in sst (sstfront) and mixed layer height (mid). The dependent variable (BAI) was the 0.9 quantile of the integrated acoustic energy observations in the "virgin" sequence.

Figure 7, Figure 8 and Figure 9 show boxplots of log transformed BAI nominal values for each of the independent variables, expressed as categorical. Figure 10 shows the quarterly evolution of the log BAI index by squares of 5x5 degrees from 2010 to 2018.

The results of the deviance analysis are shown in Table 1. The model explained 24% of the total deviance being the most significant explanatory factors: year-quarter, 5°x5° area and the interaction year-quarter\*area that was considered as random interaction. No significant residual patterns were observed (Figure 11).

Quarterly series of standardized BAI index are provided in Table 2 and Figure 12. Most of the nominal values are embedded within the confidence interval of the standardized BAI index. The BAI index shows that there is a relative stability over the period analysed. However, three different stanzas can be clearly identified: a) an initial period, between the first quarter of 2010 and the third quarter of 2012, with an average BAI value of 2,67; b) a period of relatively higher values from the fourth quarter of 2012 to the fourth quarter of 2015 (BAI=4.22) and c) a final period of relatively lower values (BAI=1.88). The first two periods showed a clear inter-quarter variability, while the later was relatively more stable. Coefficients of variation were higher at the beginning of the series, between 0.26 and 1.20 in 2010-2012, decreasing to values between 0.12 and 0.26 for the rest of the series.

## **Acknowledgements**

This work was supported by the Government of the Basque Country and the EU funded projects RECOLAPE and CECOFAD2. We thank the Spanish vessel owner associations ANABAC and OPAGAC and those companies that have provided acoustic information from their echosounder buoys were: Albacora, Atunsa, Atunsa INC, Comp Europea de Tunidos, Echebatar fleet, Hartswater, Inpesca, Inpesca Fishing, Interatun and Isabella Fishing. We are also thankful to the three buoy providers companies Marine Instruments, Satlink and Zunibal.

## References

- Bates, D., Mächler, M., Bolker, B., & Walker, S. (2015). Fitting Linear Mixed-Effects Models Using lme4. *Journal of Statistical Software*, 67(1), 1–48. <https://doi.org/10.18637/jss.v067.i01>
- Belkin, I. M., & O'Reilly, J. E. (2009). An algorithm for oceanic front detection in chlorophyll and SST satellite imagery. *Journal of Marine Systems*, 78, 319–326. <https://doi.org/10.1016/j.jmarsys.2008.11.018>
- Boyra, G., Moreno, G., Sobradillo, B., Pe, I., Sancristobal, I., & Demer, D. A. (2018). Target strength of skipjack tuna (*Katsuwonus pelamis*) associated with fish aggregating devices (FADs). *ICES Journal of Marine Science*, 75, 1790–1802. <https://doi.org/10.1093/icesjms/fsy041>
- Brill, R. V., Block, B. A., Boggs, C. H., Bigelow, K., Freund, E. V., & Marcinek, D. J. (1999). Horizontal movements and depth distribution of large adult yellowfin tuna (*Thunnus albacares*) near the Hawaiian Islands, recorded using ultrasonic telemetry: implications for the physiological ecology of pelagic fishes. *Marine Biology*, 133, 395–408.
- Dagorn, L., Holland, K., Puente, E., Taquet, M., Ramos, A., Brault, P., ... Aumeeruddy, R. (2006). *FADIO (Fish Aggregating Devices as Instrumented Observatories of pelagic ecosystems): a European Union funded project on development of new observational instruments and the behavior of fish around drifting FADs* (No. IOTC-2006-WPTT-16).
- Foote, K. G. (1983). Linearity of fisheries acoustics, with addition theorems. *The Journal of the Acoustical Society of America*, 73(6), 1932–1940. <https://doi.org/10.1121/1.389583>
- Gaertner, D., Ariz, J., Bez, N., Clermidy, S., Moreno, G., Murua, H., & Soto, M. (2016). Objectives and first results of the CECOFAFAD project. *Collect. Vol. Sci. Pap. ICCAT*, 72(2), 391–405.
- Gaertner, Daniel, Ariz, J., Bez, N., Clermidy, S., Moreno, G., Murua, H., ... Marsac, F. (2016). *Results achieved within the framework of the EU research project: Catch, Effort, and eCOsystem impacts of FAD-fishing (CECOFAFAD)* (No. IOTC-2016-WPTT18-35).
- Guéry L., Deslias C., Kaplan D., Marsac F., Abascal F., Pascual P., and Gaertner D., 2019. Accounting for fishing days without set in the CPUE standardisation of yellowfin tuna in free schools for the EU purse seine fleet operating in the Eastern Atlantic Ocean during the 1991- 2018 period. SCRS/2019/066.
- Hampton, I. (1996). Acoustic and egg-production estimates of South African anchovy biomass over a decade: comparisons, accuracy, and utility. *ICES Journal of Marine Science*, 53(2), 493–500. <https://doi.org/10.1006/jmsc.1996.0071>
- Hoyle, S. D., Huang, J. H., Kim, D. N., Lee, M. K., Matsumoto, T., & III, J. W., 2019. Standardization of bigeye tuna CPUE in the Atlantic Ocean by the Japanese longline fishery which includes cluster analysis. *Collect. Vol. Sci. Pap. ICCAT*, 75(7), 2098–2116.
- Hoyle S.D., Lauretta M., Lee M.K., Matsumoto T., Sant'Ana R., and Yokoi H., 2019. Collaborative study of yellowfin tuna CPUE from multiple Atlantic Ocean longline fleets in 2019. SCRS/2019/081.
- ICCAT 2019a. Report of the 2019 ICCAT yellowfin tuna data preparatory meeting (Madrid, Spain, 22-26 April 2019)
- ICCAT 2019b. Report of the 2019 ICCAT yellowfin tuna stock assessment meeting (Grand Bassam, Ivory Coast, 8-16 July 2019).
- ICES. (2015). *Manual for International Pelagic Surveys (IPS)*. Copenhagen.
- Josse, E., Bach, P., & Dagorn, L. (1998). Simultaneous observations of tuna movements and their prey by sonic tracking and acoustic surveys. In *Advances in Invertebrates and Fish Telemetry* (pp. 61–69). [https://doi.org/10.1007/978-94-011-5090-3\\_8](https://doi.org/10.1007/978-94-011-5090-3_8)
- Lo, N. C., Jacobson, L. D., & Squire, J. L. (1992). Indices of Relative Abundance from Fish Spotter Data based on Delta-Lognormal Models. *Canadian Journal of Fisheries and Aquatic Sciences*, 49(12), 2515–2526.
- Lopez, J., Moreno, G., Ibaibarriaga, L., & Dagorn, L. (2017). Diel behaviour of tuna and non-tuna species at drifting fish aggregating devices (DFADs) in the Western Indian Ocean, determined by fishers' echo-sounder buoys. *Marine Biology*, 164(3), 44. <https://doi.org/10.1007/s00227-017-3075-3>
- Lopez, J., Moreno, G., Sancristobal, I., & Murua, J. (2014). Evolution and current state of the technology of echo-sounder buoys used by Spanish tropical tuna purse seiners in the Atlantic, Indian and Pacific Oceans. *Fisheries Research*, 155, 127–137. <https://doi.org/10.1016/j.fishres.2014.02.033>



- MacLennan, D., Fernandes, P. G., & Dalen, J. (2002). A consistent approach to definitions and symbols in fisheries acoustics. *ICES Journal of Marine Science*, 59(2), 365–369. <https://doi.org/10.1006/jmsc.2001.1158>
- Massé, J., Uriarte, A., Angélico, M. M., & Carrera, P. (2018). *Pelagic survey series for sardine and anchovy in ICES subareas 8 and 9 – Towards an ecosystem approach*.
- Maunder, M. N., & Punt, A. E. (2004). Standardizing catch and effort data: a review of recent approaches. *Fisheries Research*, 70(2–3), 141–159. <https://doi.org/10.1016/j.fishres.2004.08.002>
- Maunder, M. N., Sibert, J., Fonteneau, A., Hampton, J., Kleiber, P., & Harley, S. J. (2006). Interpreting catch per unit effort data to assess the status of individual stocks and communities. *ICES Journal of Marine Science*, 63(8), 1373–1385. <https://doi.org/10.1016/j.icesjms.2006.05.008>
- Methot, R. D., & Wetzel, C. R. (2012). Stock synthesis: A biological and statistical framework for fish stock assessment and fishery management. *Fisheries Research*. <https://doi.org/10.1016/j.fishres.2012.10.012>
- Moreno, G., Boyra, G., Sancristobal, I., & Restrepo, V. (2019). Towards acoustic discrimination of tropical tunas associated with Fish Aggregating Devices. *PloS ONE*, 14(6), 24. <https://doi.org/https://doi.org/10.1371/journal.pone.0216353>
- Moreno, Gala, Dagorn, L., Sancho, G., & Itano, D. (2007). Fish behaviour from fishers' knowledge: the case study of tropical tuna around drifting fish aggregating devices (DFADs). *Canadian Journal of Fisheries and Aquatic Sciences*, 64(11), 1517–1528. <https://doi.org/10.1139/f07-113>
- Murua, Hilario et al. 2017. "Fast versus Slow Growing Tuna Species: Age, Growth, and Implications for Population Dynamics and Fisheries Management." *Reviews in Fish Biology and Fisheries* 27(4): 733–73.
- Orue, B., Lopez, J., Moreno, G., Santiago, J., Soto, M., & Murua, H. (2019). Aggregation process of drifting fish aggregating devices (DFADs) in the Western Indian Ocean: Who arrives first, tuna or non-tuna species? *Plos One*, 14(1), e0210435. <https://doi.org/10.1371/journal.pone.0210435>
- Oshima, T. (2008). *Target strength of Bigeye, Yellowfin and Skipjack measured by split beam echo sounder in a cage*. Indian Ocean Tuna Commission Working Party on Tropical Tunas. (No. WPTT-22).
- Punt, A. E., Walker, T. I., Taylor, B. L., & Pribac, F. (2000). Standardization of catch and effort data in a spatially-structured shark fishery. *Fisheries Research*, 45(2), 129–145. [https://doi.org/10.1016/S0165-7836\(99\)00106-X](https://doi.org/10.1016/S0165-7836(99)00106-X)
- Quinn, T. J., & Deriso, R. B. (Richard B. . (1999). *Quantitative fish dynamics*. Retrieved from [https://books.google.es/books/about/Quantitative\\_Fish\\_Dynamics.html?id=5FVBj8jnh6sC&redir\\_esc=y](https://books.google.es/books/about/Quantitative_Fish_Dynamics.html?id=5FVBj8jnh6sC&redir_esc=y)
- Robert, M., Dagorn, L., Lopez, J., Moreno, G., & Deneubourg, J.-L. (2013). Does social behavior influence the dynamics of aggregations formed by tropical tunas around floating objects? An experimental approach. *Journal of Experimental ...*, 440, 238–243. Retrieved from <http://www.sciencedirect.com/science/article/pii/S0022098113000099>
- Røttingen, I. (1976). On the relation between echo intensity and fish density. *FiskDir. Skr. Ser. Havunders.*, 16(9), 301–314. Retrieved from <https://brage.bibsys.no/xmlui/handle/11250/114400>
- Santiago, J., Lopez, J., Moreno, G., Murua, H., Quincoces, I., & Soto, M. (2016). Towards a tropical tuna buoy-derived abundance index (TT-BAI). *Collect. Vol. Sci. Pap. ICCAT*, 72(3), 714–724.
- Scott, G. P., & Lopez, J. (2014). *The use of FADs in Tuna Fisheries*. European Parliament. Policy Department B: Structural and Cohesion Policies: Fisheries. IP/B/PECH/IC/2013.
- Simmonds, E. J., & MacLennan, D. N. (2005). *Fisheries acoustics : theory and practice*. Blackwell Science.
- Torres-Irineo, E., Gaertner, D., Chassot, E., & Dreyfus-León, M. (2014). Changes in fishing power and fishing strategies driven by new technologies: The case of tropical tuna purse seiners in the eastern Atlantic Ocean. *Fisheries Research*, 155, 10–19. <https://doi.org/10.1016/j.fishres.2014.02.017>

Variable	Df	Deviance	Resid..Df	Resid..Dev	F	Pr..F.	Dev..Exp
NULL	NA	NA	28299	83178	NA	NA	
yyqq	35	8546	28264	74632	106	0.00E+00	10.27%
area	21	1899	28243	72734	39	1.29E-158	2.28%
model	3	82	28240	72652	12	8.94E-08	0.10%
den	1	4	28239	72648	2	2.06E-01	0.00%
chl	1	153	28238	72495	67	3.39E-16	0.18%
chlfront	1	2	28237	72493	1	3.57E-01	0.00%
sst	1	6	28236	72487	2	1.16E-01	0.01%
sstfront	1	58	28235	72429	25	5.06E-07	0.07%
mld	1	150	28234	72278	65	6.39E-16	0.18%
yyqq:area	495	5803	27739	66476	5	7.11E-253	6.98%
yyqq:model	26	738	27713	65738	12	3.30E-52	0.89%
yyqq:chl	35	808	27678	64930	10	1.97E-53	0.97%
yyqq:chlfront	34	224	27644	64706	3	4.97E-08	0.27%
yyqq:sst	32	587	27612	64118	8	2.04E-36	0.71%
yyqq:sstfront	31	133	27581	63985	2	2.44E-03	0.16%
yyqq:mld	30	455	27551	63531	7	1.78E-26	0.55%
yyqq:den	30	213	27521	63318	3	2.75E-08	0.26%

Table 1. Deviance table for the GLM lognormal model of the 2010-2018 period. Significant ( $p < 0.05$ ) factors and interactions explaining >5% of total deviance are highlighted.

Quarter	Index nominal	BAI Index	BAI se	BAI cv	Quarter	Index nominal	BAI Index	BAI se	BAI cv
<b>10Q1</b>	1.324	1.351	0.696	0.515	<b>14Q3</b>	2.344	2.388	0.430	0.180
<b>10Q2</b>	2.147	2.472	1.788	0.724	<b>14Q4</b>	7.098	6.350	0.933	0.147
<b>10Q3</b>	2.323	2.679	0.800	0.299	<b>15Q1</b>	3.352	3.472	0.532	0.153
<b>10Q4</b>	3.252	5.149	4.530	0.880	<b>15Q2</b>	7.461	4.605	0.794	0.172
<b>11Q1</b>	2.286	2.190	0.889	0.406	<b>15Q3</b>	6.033	5.608	0.834	0.149
<b>11Q2</b>	2.172	2.606	3.140	1.205	<b>15Q4</b>	2.145	2.082	0.289	0.139
<b>11Q3</b>	3.225	3.675	1.757	0.478	<b>16Q1</b>	1.503	1.574	0.226	0.144
<b>11Q4</b>	2.857	3.389	2.008	0.593	<b>16Q2</b>	1.613	1.406	0.233	0.166
<b>12Q1</b>	1.802	1.505	0.563	0.374	<b>16Q3</b>	2.109	2.233	0.333	0.149
<b>12Q2</b>	2.126	2.136	0.663	0.310	<b>16Q4</b>	2.068	2.083	0.252	0.121
<b>12Q3</b>	2.197	2.253	0.594	0.264	<b>17Q1</b>	1.521	1.382	0.220	0.159
<b>12Q4</b>	6.059	6.162	1.636	0.265	<b>17Q2</b>	1.929	1.919	0.288	0.150
<b>13Q1</b>	3.601	2.733	0.589	0.215	<b>17Q3</b>	1.794	1.845	0.318	0.173
<b>13Q2</b>	6.857	4.769	0.901	0.189	<b>17Q4</b>	1.821	1.939	0.358	0.184
<b>13Q3</b>	3.798	3.741	0.749	0.200	<b>18Q1</b>	1.634	1.437	0.251	0.175
<b>13Q4</b>	7.366	6.131	1.087	0.177	<b>18Q2</b>	2.022	1.934	0.339	0.175
<b>14Q1</b>	3.641	3.076	0.581	0.189	<b>18Q3</b>	2.641	2.907	0.487	0.168
<b>14Q2</b>	5.873	3.860	0.692	0.179	<b>18Q4</b>	1.895	1.848	0.384	0.208

Table 2. Nominal and standardized Buoy-derived Abundance Index for the period 2010-2018. Standard errors and coefficient of variations of the standardized series are also included.

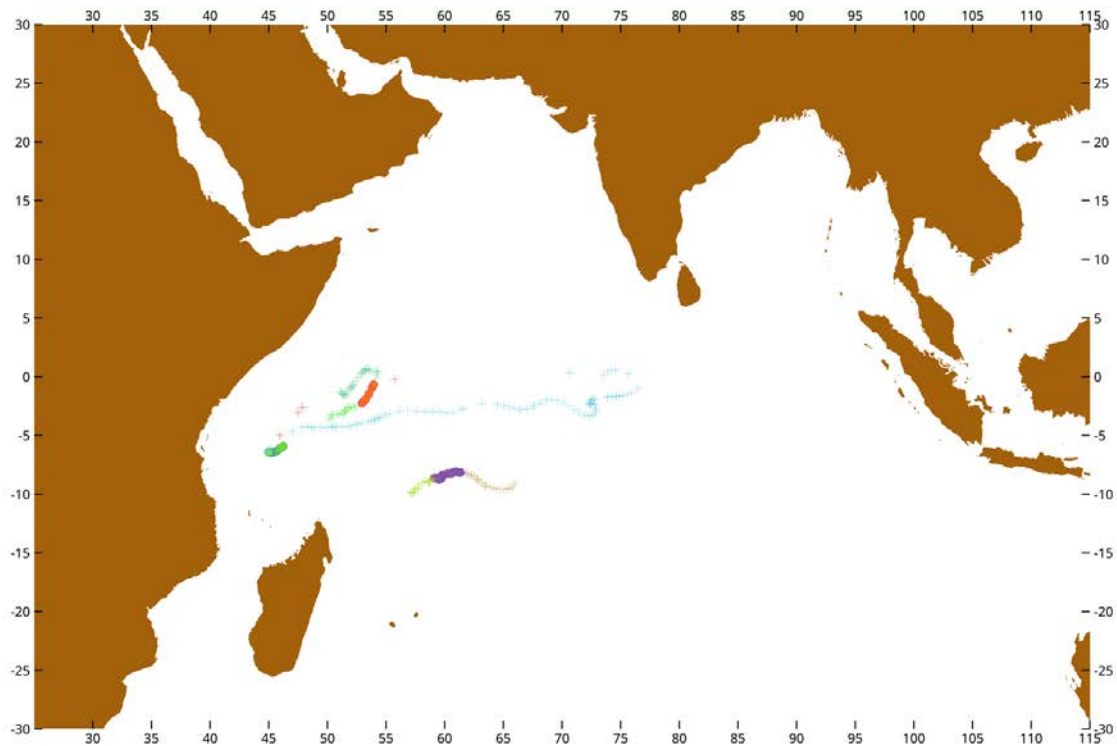
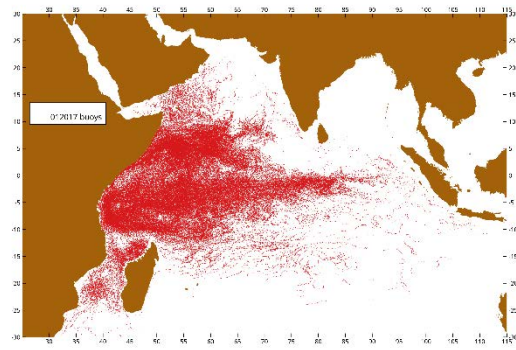
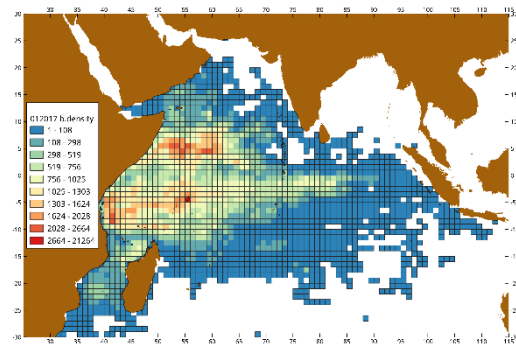


Figure 1. Example of “virgin” segments used for the calculation of the BAI index. Trajectories correspond to buoy ISL+151350 with four different paths representing drifts of different FADs. A virgin segment is defined as the segment of a buoy trajectory whose associated FAD likely represents a new deployment, which has been potentially colonized by tuna and not already fished. We consider as virgin segments (i.e. when tuna has aggregated to FAD) those segments of trajectories from 20-35 days at sea. In this figure, “Virgin” segments are represented as thick points in each trajectory.

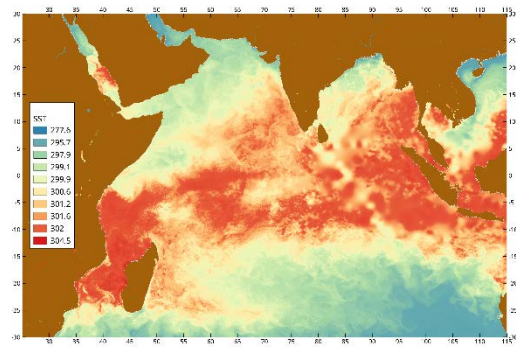
## Trajectories



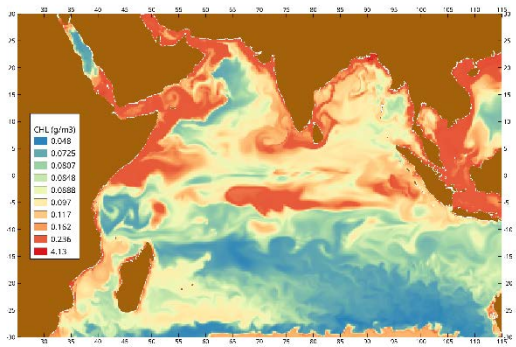
## Densities



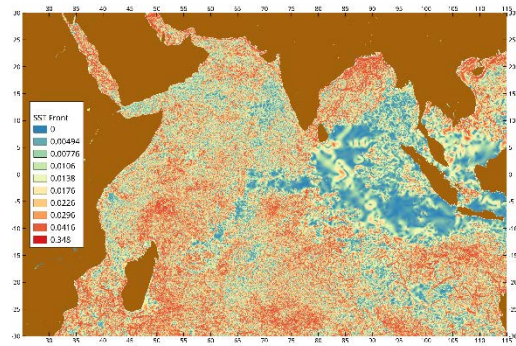
## Sea surface temperature (SST)



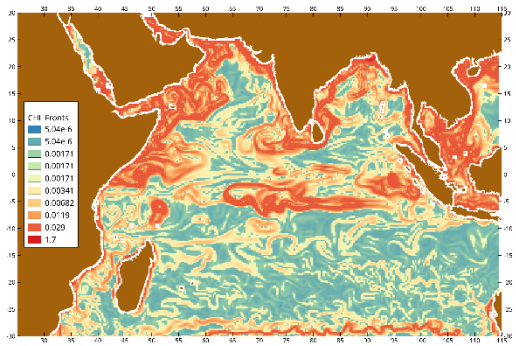
## Chlorophyll concentration



## SST fronts



## Chlorophyll fronts



## Mixed layer height

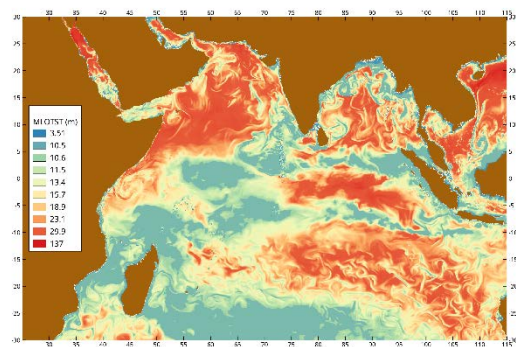


Figure 2. Example of one month of data, January 2017, of buoy trajectories, density of buoys by 1°x1° and environmental variables incorporated in the GLM analysis: sea surface temperature (SST), chlorophyll concentration, detected fronts in SST, detected fronts in chlorophyll and mixed layer height.

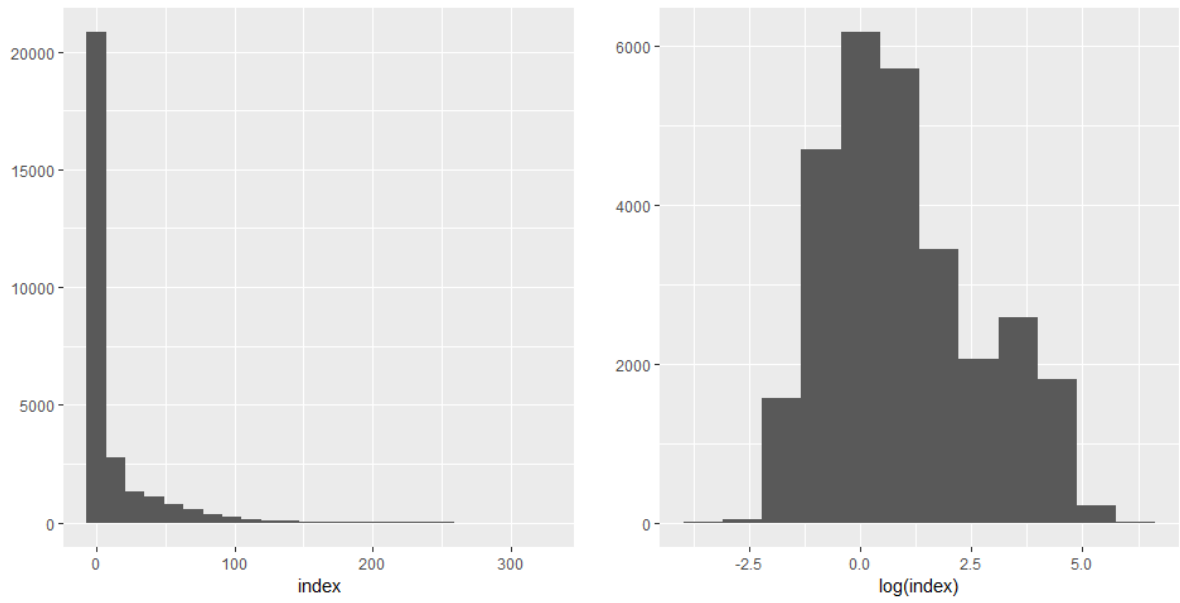


Figure 2. Histograms of the nominal values (left) and the log transformed nominal values (right) of the Buoy-derived Abundance Index (0.9 quantile of the integrated acoustic energy observations in "virgin" sequences).

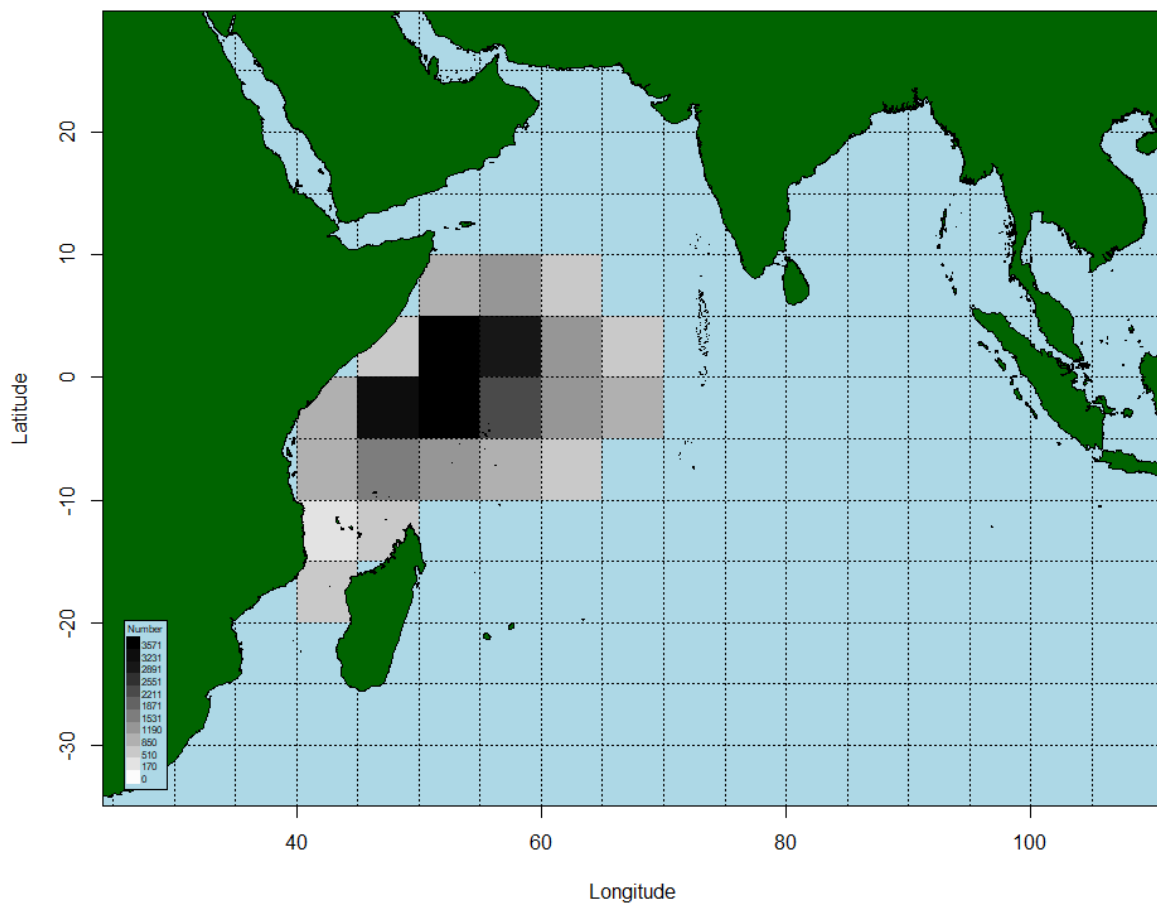


Figure 3. Spatial distribution [5°x5°] of the "virgin" sequences of buoy trajectories that have been used in the GLM analysis.

## Number of observations

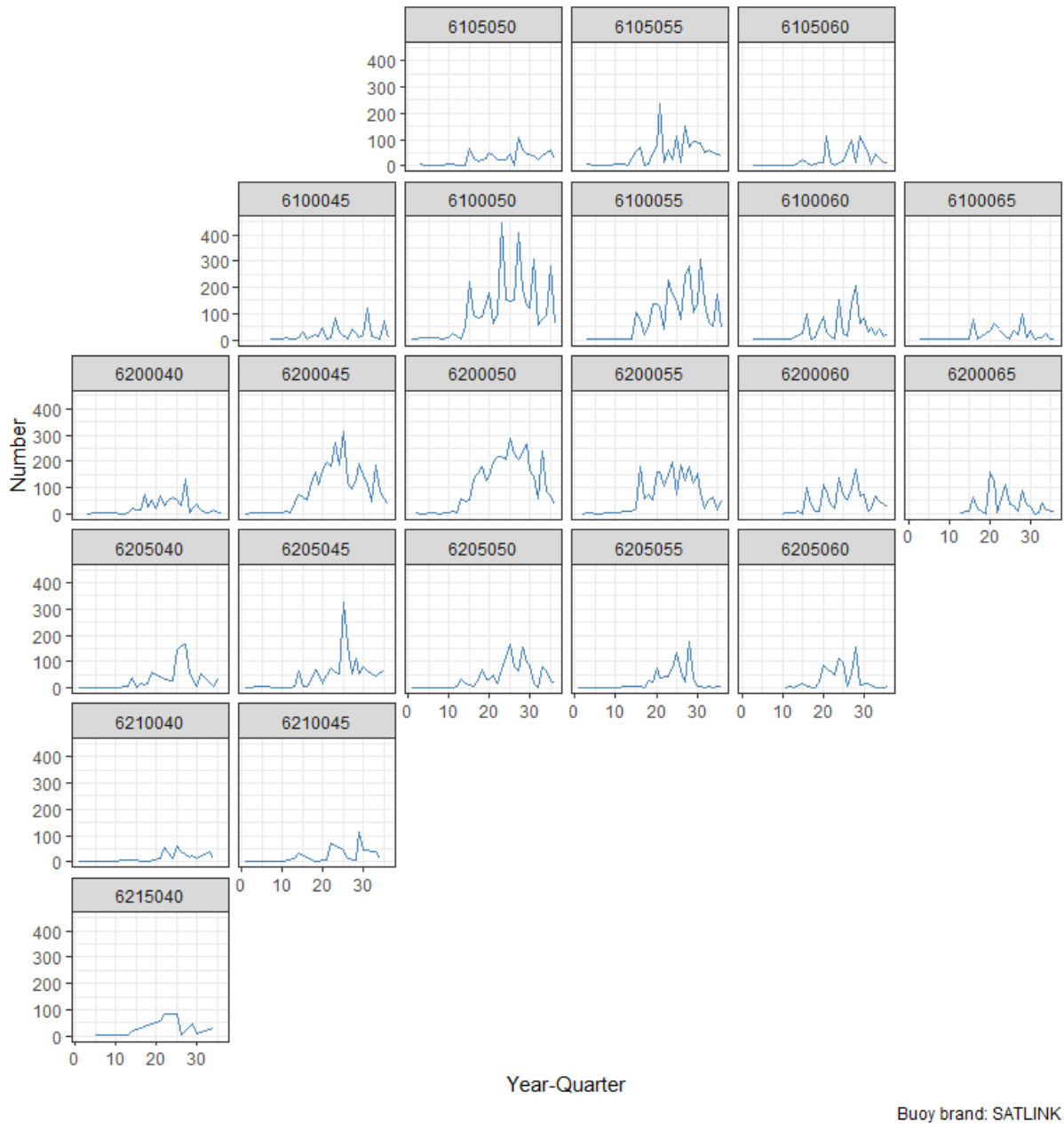


Figure 4. Quarterly evolution of the number of observations ("virgin" sequences of buoy trajectories) on a  $5^{\circ} \times 5^{\circ}$  grid.

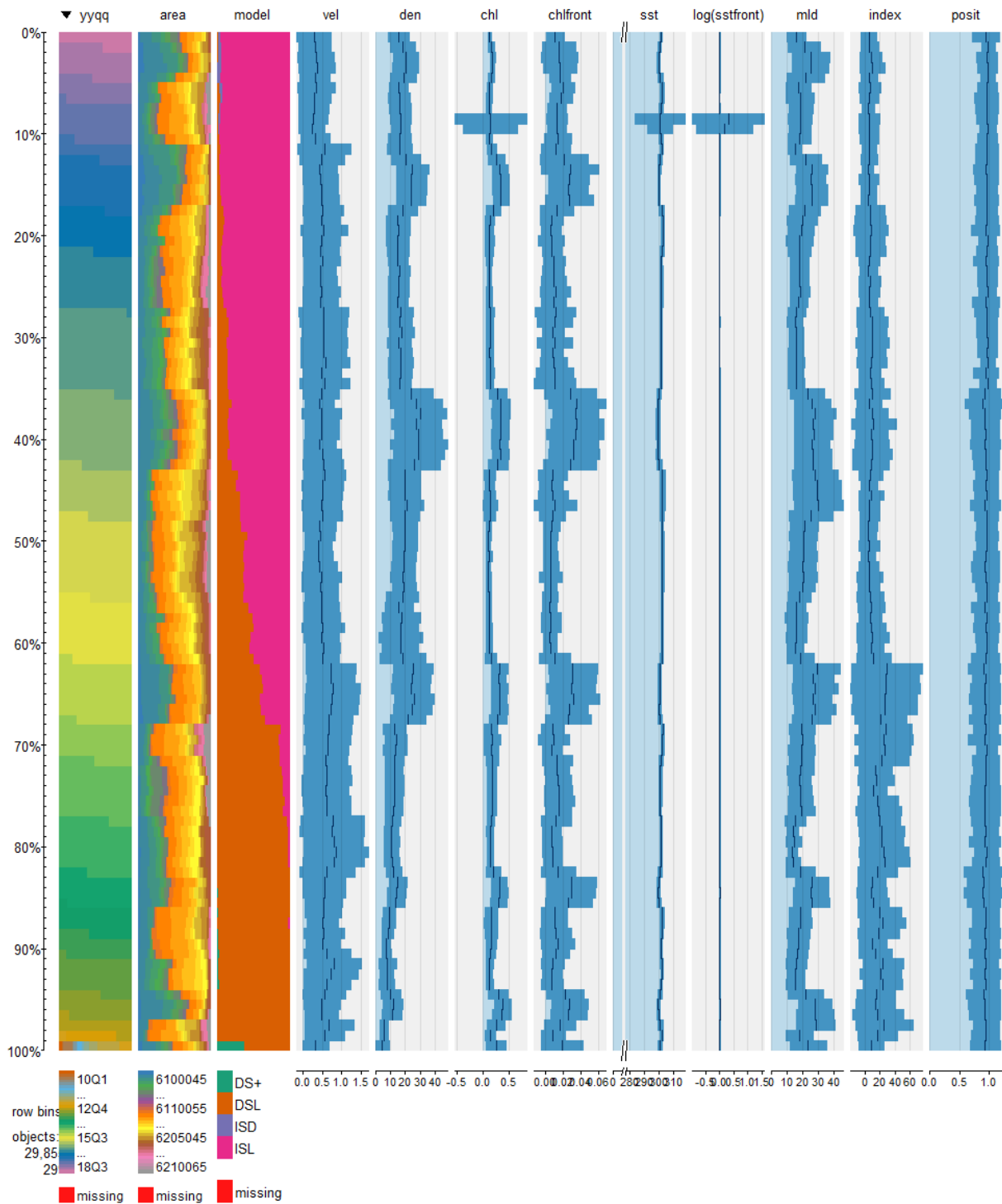
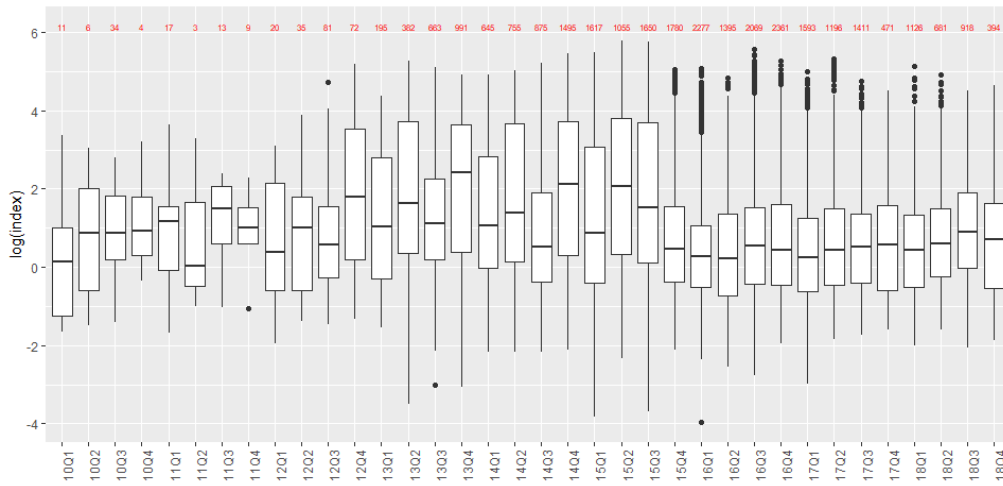
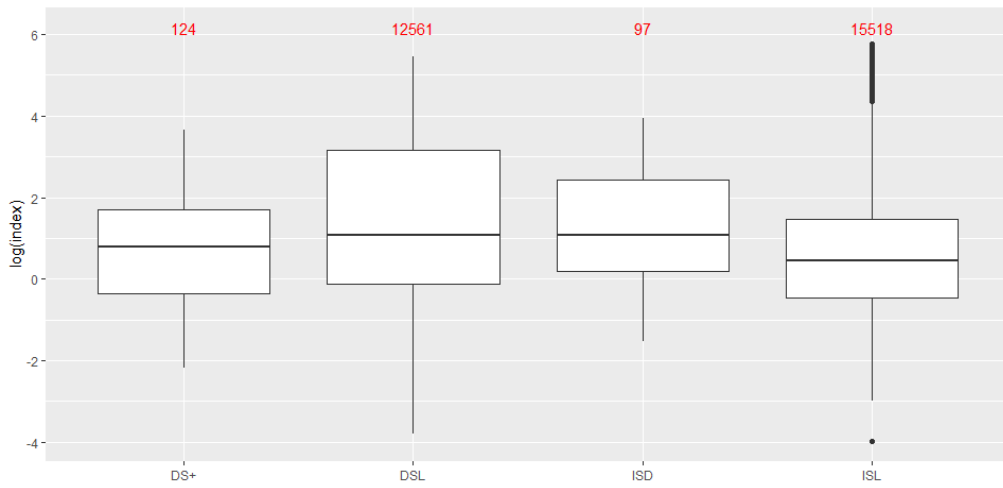


Figure 5. Tableplot of the variables used in the GLM analysis. Each column represents a variable and each row bin is an aggregate of a certain number of records. For numeric variables, a bar chart of the mean values is depicted. For categorical variables, a stacked bar chart is depicted of the proportions of categories. Independent variables tested in the GLM were year-quarter (yyqq), 5°x5° area (area), buoy model (model), buoy velocity (vel), FAD density (den), chlorophyll concentration (chl), detected fronts in chlorophyll (chlfront), sea surface temperature (SST), detected fronts in SST (sstfront) and mixed layer height (mld). The dependent variable for the lognormal component was the 0.9 quantile of the integrated acoustic energy observations in the "virgin" sequence (index); and for the binomial component, the proportion of positives (posit).

A) Year-quarter



B) Buoy model



C) Buoy speed

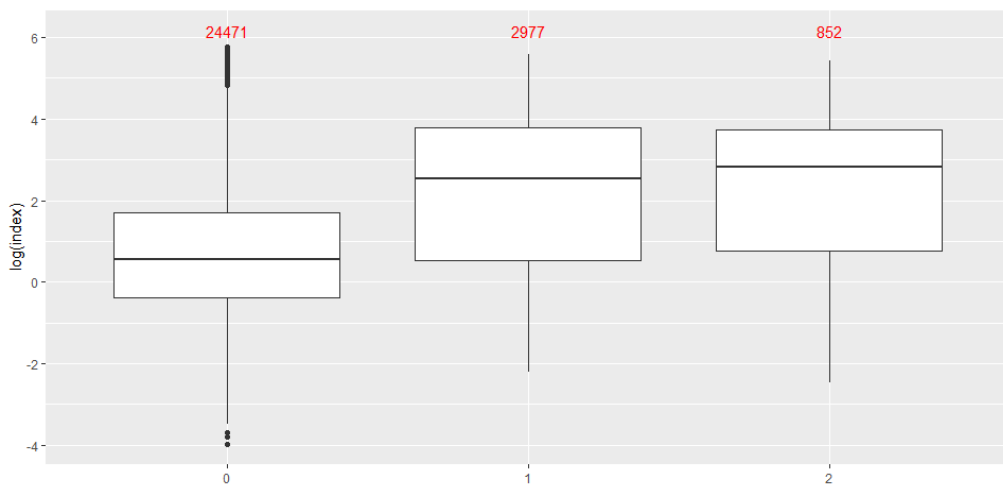
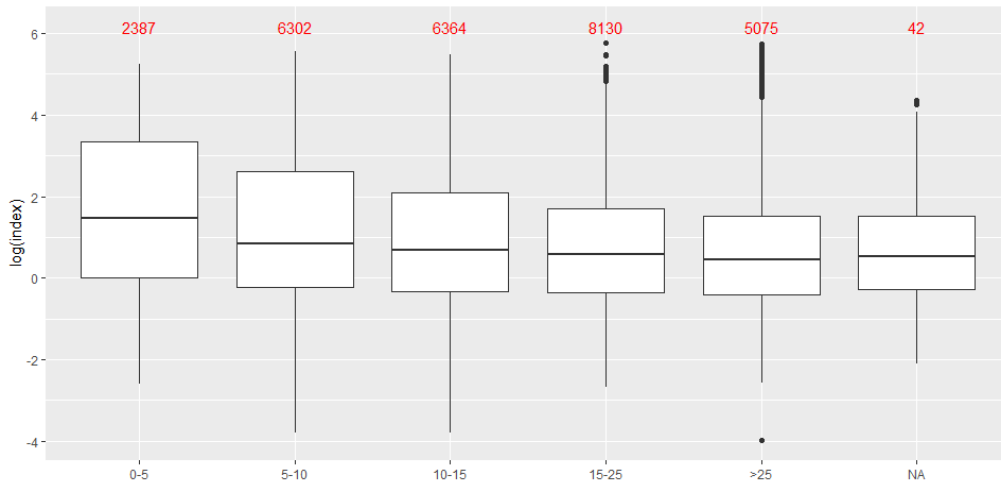


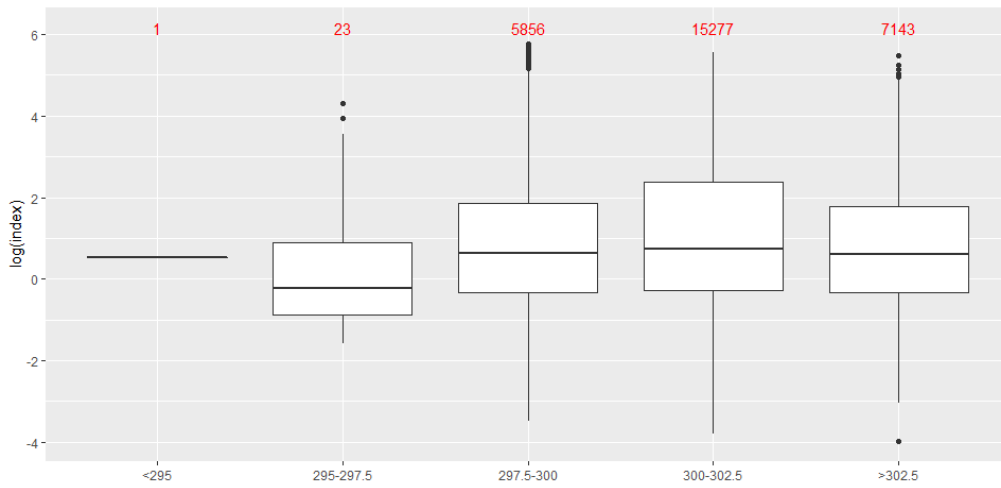
Figure 6. Boxplot of  $\log(\text{BAI})$  for year-quarter, buoy model and buoy speed (expressed as categorical). Number of observations for each categorical value is shown in red.



### A) Buoy densities



### B) Sea surface temperature



### C) Chlorophyll concentration

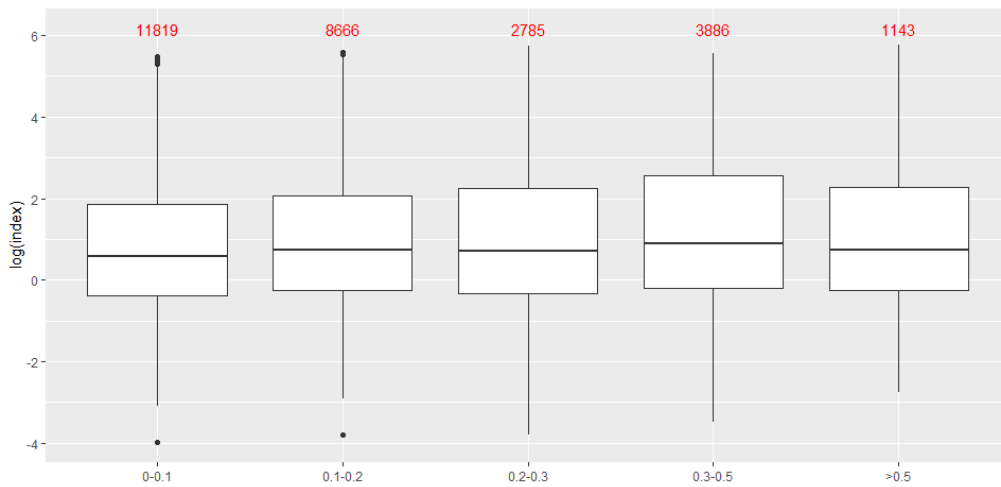
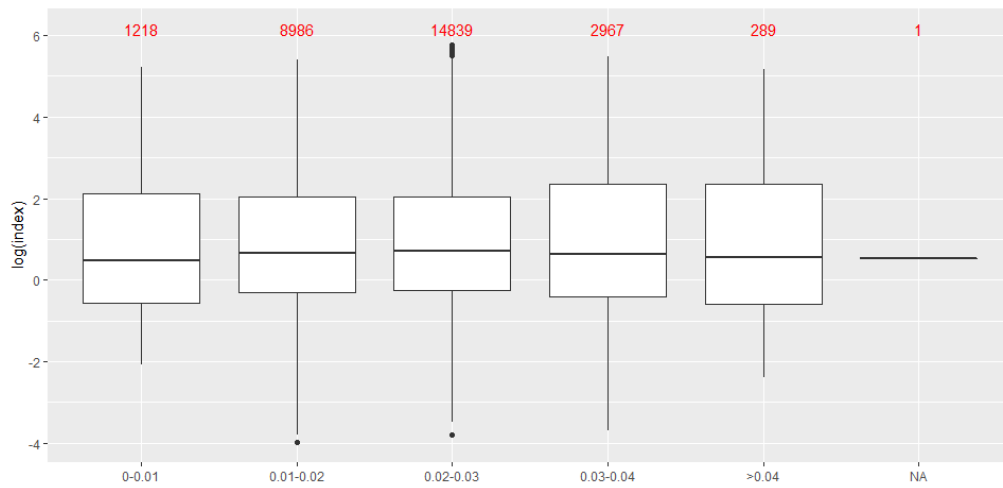
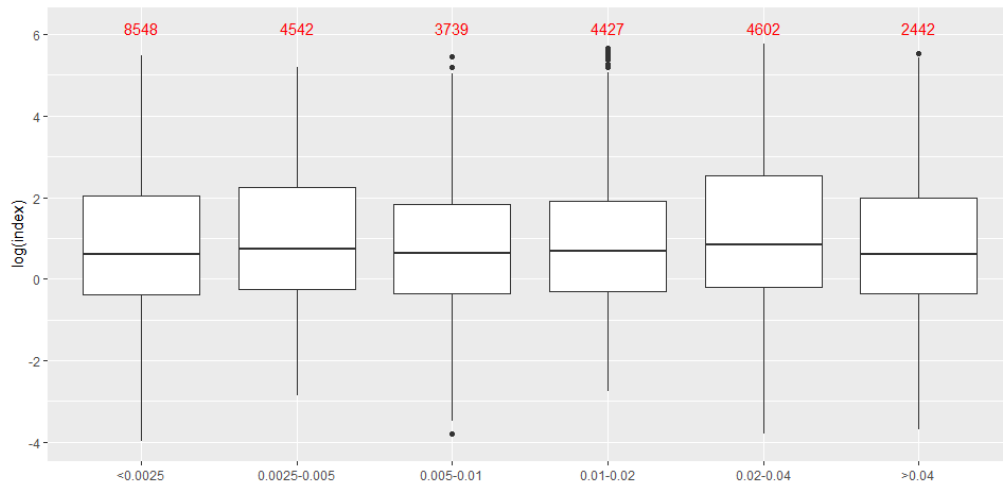


Figure 7. Boxplot of log (BAI) for buoy densities, sea surface temperature and chlorophyll concentration (expressed as categorical). Number of observations for each categorical value is shown in red.

### A) Fronts of sea surface temperature



### B) Fronts of chlorophyll concentration



### C) Mixed layer height

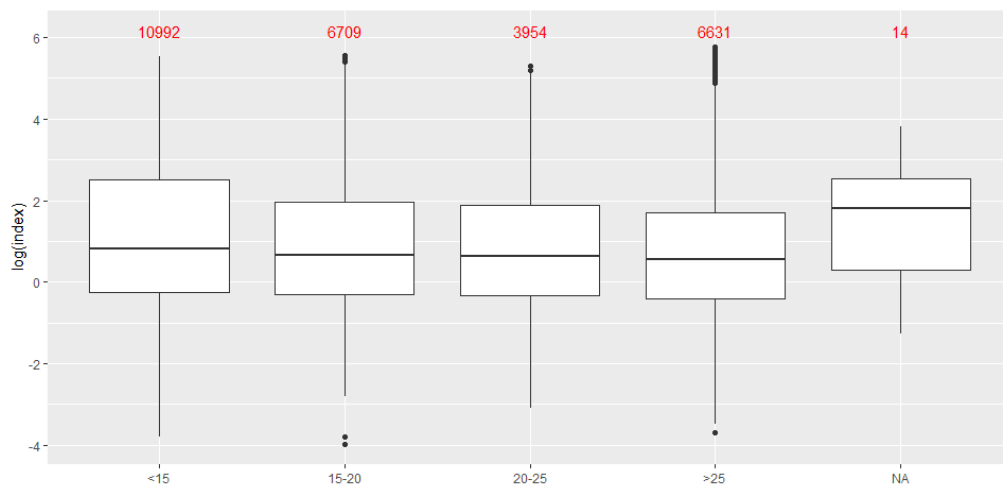


Figure 8. Boxplot of  $\log(\text{BAI})$  for fronts of sea surface temperature, fronts of chlorophyll concentration and mixed layer height (expressed as categorical). Number of observations for each categorical value is shown in red.

Positive values [log biomass]

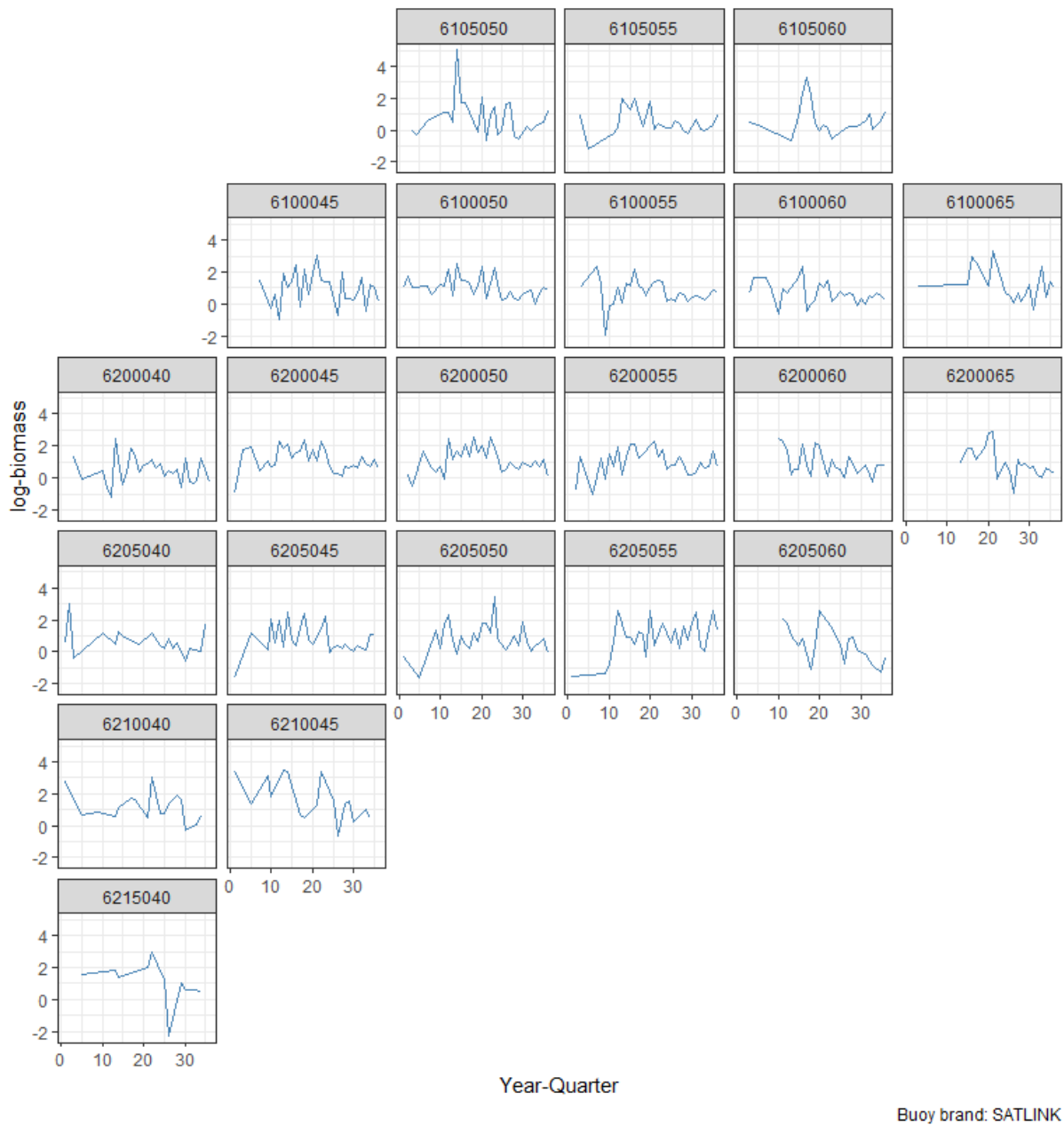


Figure 9. Quarterly evolution of the log BAI index in the Indian Ocean by squares of 5x5 degrees from 2010 to 2018.

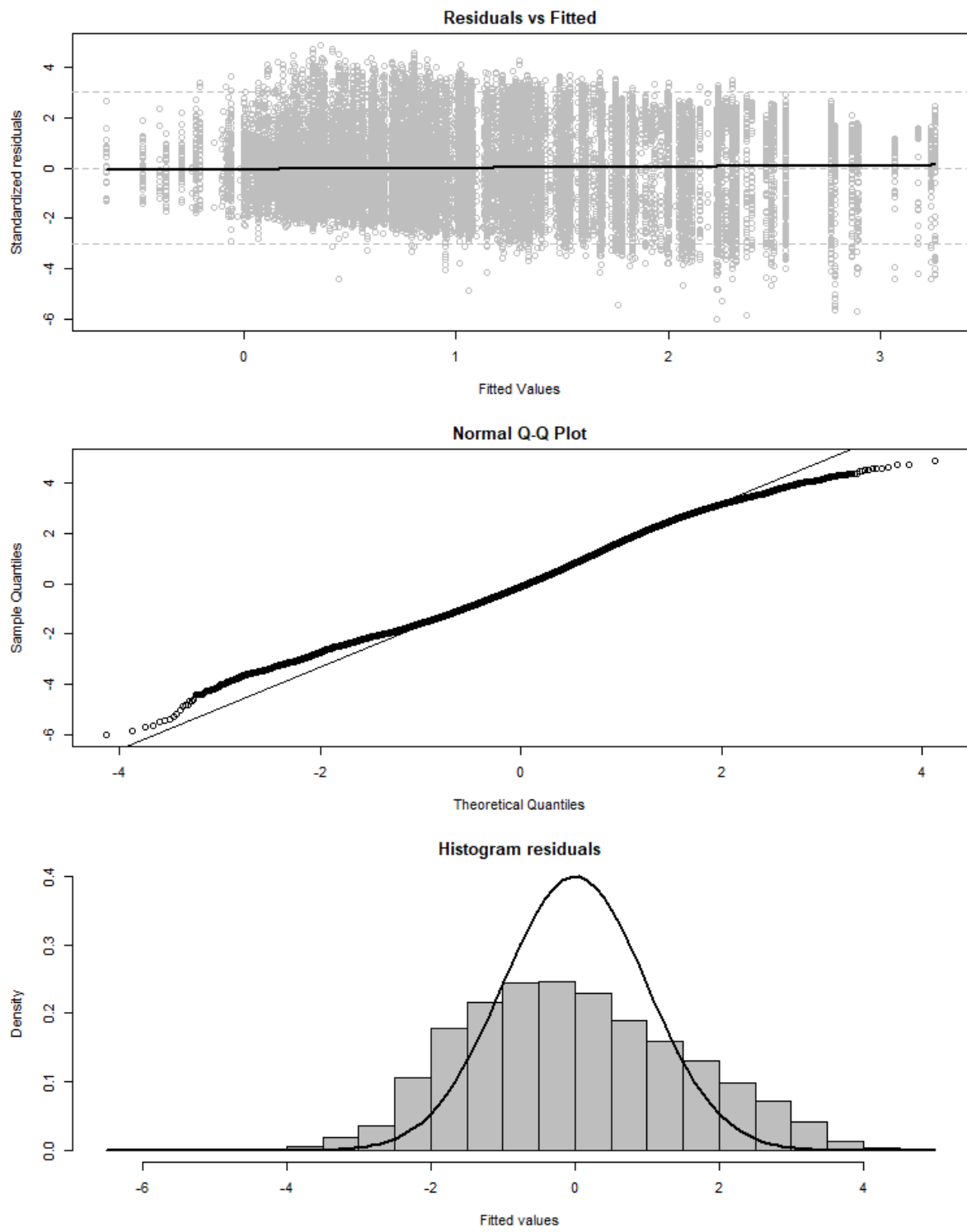


Figure 10. Diagnostics of the lognormal model selected for the period 2010-2018: residuals vs fitted, Normal Q-Q plot and frequency distributions of the residuals.

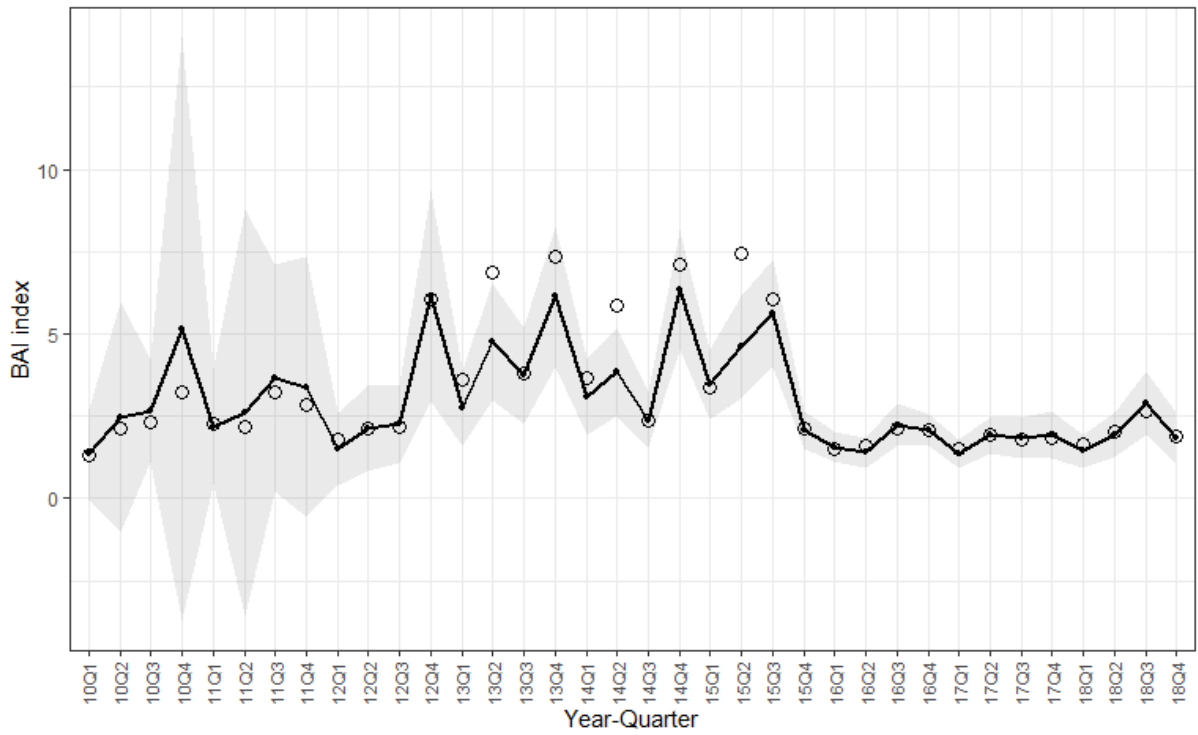


Figure 11. Time series of nominal (circles) and standardized (continuous line) Buoy-derived Abundance Index for the period 2010-2018. The 95% upper and lower confidence intervals of the standardized BAI index are shown.